Desalination and Water Treatment
www.deswater.com

doi: 10.5004/dwt.2022.28935

276 (2022) 62–69
November

Comparative study of commercially available biomimetic membrane performance for seawater desalination

Ahmed Al-Sairafi, Garudachari Bhadrachari*, Mansour Ahmed, Safeyah B. Al-Muqahwi, Mansour Al-Rughaib

Kuwait Institute for Scientific Research, Water Research Center, P.O. Box: 24885, Safat 13109, Kuwait, emails: bgarudachari@kisr.edu.kw (G. Bhadrachari), asairafy@kisr.edu.kw (A. Al-Sairafi), mahmed@kisr.edu.kw (M. Ahmed), smuqahwi@kisr.edu.kw (S.B. AL-Muqahwi), mrughaib@kisr.edu.kw (M. Al-Rughaib)

Received 23 June 2022; Accepted 23 September 2022

ABSTRACT

Desalination using forward osmosis (FO) is one of the low energy separation processes. The driving force for this separation is the osmotic pressure difference between feed solution (FS) and draw solution (DS) between the semipermeable polymer membrane. In recent years, the economic and technical feasibility of FO process for desalination application has attracted scientists from various disciplines, including water purification, desalination, and power generation. On the other hand, biologically, inspired membranes called aquaporin/biomimetic membrane showed promising results in separation process with lower energy consumption. Therefore, the study was conducted to evaluate and compare the desalination performance of the commercially available aquaporin membranes in FO process. The aim of this study was to assess and compare the viability and efficiency of the commercially available biomimetic membranes namely biomimetic aquaporin and Z-nano membranes in laboratory bench-scale test unit for desalinating different concentration of saline waters. The study was conducted by varying the operating parameters such as flow rate, temperature and concentration of feed and DS. The seawater desalination study showed maximum water flux of 57.9 and 23.7 L/m^2·h for seawater and reverse osmosis brine FS, respectively using 26 wt.% sodium chloride DS and Z-nano membrane. The optimum operating conditions observed was flow rate of 500 mL/min and 25°C temperature. Comparatively, Z-nano membranes showed better desalination performance than biomimetic aquaporin for all the tested FS, DS and operating conditions.

Keywords: Seawater desalination; Brine concentration; Water recovery; Salt rejection

1. Introduction

The Gulf Cooperation Council (GCC) countries are situated in the southwestern region of the Asian continent. The most of the land in GCC is arid with dry climate, short winter and limited underground freshwater resources [1,2]. The GCC countries relay on desalination process to manage their freshwater demands. The main desalination processes are thermal multi-stage flash (MSF) and membrane based reverse osmosis (RO) technologies [3,4]. Kuwait seawater is characterized by increased salinity and turbidity. The aforementioned thermal and membrane-based desalination technologies are energy intensive and having fouling, scaling issues due to higher salinity of seawater [5–7]. In recent years, forward osmosis (FO) process showed promising results in laboratory scale and pilot scale for seawater desalination application with low energy consumption. FO works under natural osmosis process, the high osmotic pressure draw solution (DS) selectively extract the water molecules from the contaminated water/seawater through

* Corresponding author.

the membrane due to osmotic pressure difference. The principle of FO technology for desalination application consists of two stages to generate pure water. First stage is actual membrane separation process and the second stage is regeneration of DS by thermal or membrane process [8]. Due to the lack of an efficient FO membrane for the desalination process, the proof of the commercial viability of the technology is still in its infancy. In recent years, new membrane has been developed by incorporating transmembrane proteins, known as aquaporins (AQP), which has a potential of water separation from saline/waste water [9–11]. The Peter Agre in 1992 found that the biological membranes provide solid molecular evidence for achieving higher water flux and higher salt rejection [12–18]. The AQP are biological membrane proteins for water transport in biological cells of bacteria, fungi, animal, and plant cells. The AQP has higher water permeability in the range of four billion water molecules per second which is mainly due to the protein structural orientation and chemical identities. AQP protein has size restriction water channel with polar and non-polar chemical functional groups which will create the electrostatic attraction and repulsion during the water transportation. Therefore, there is huge scape for conducting desalination performance study using biomimetic/AQP membranes in FO process. Recent research indicates that biomimetic membranes exhibit salt rejection greater than 96% and water permeability greater than 4 L m^2/h·bar [19]. The water flux of biomimetic membrane is two magnitudes more than that of conventional commercial RO membrane [19,20]. Madsen et al. [21] conducted study on removal of trace organics in the feed solution using newly developed biomimetic membrane. The biomimetic membrane rejected more than 97% of trace organics which was higher than the cellulose triacetate (CTA) membrane. Li et al. [20] applied biomimetic membrane for seawater desalination at 55 bar applied pressure. The study showed biomimetic membrane showed 80% higher water flux compared with commercial SW30HR membrane. The FO experimental studies of biomimetic membranes showed significantly higher separation performance compared with FO-CTA and FO-HTI (Hydration Technology Innovations, Albany, Oregon, USA) membranes [22].

Prompted by desalination performance of biomimetic/AQP protein membranes, observations and in continuation of our research on desalination using FO technology [23–27], the desalination performance of commercially available biomimetic/AQP membranes was conducted.

2. Experimental

2.1. Materials

The commercially available biomimetic/AQP membranes were purchased from Aquaporin A/S, Denmark and Z-nano Water Tech, California. The specifications of the biomimetic membranes are presented in Table 1. The chemical required for DS, feed solution (FS) preparations were purchased from Sigma-Aldrich and used without any further purification. The seawater and RO brine was collected from beach-well at the Doha Desalination Research Plant (DRP) Kuwait and the de-ionized water was collected from Siemens Ultra-Clear TWF Water Purification Systems. The major elemental composition of the seawater and seawater reverse osmosis (SWRO) brine is shown in Table 2. The laboratory scale FO instrument was purchased from Trevi Systems California and installed at DRP. The trial runs were conducted to ensure that the overall performance is in-line with the required parameters, specifications of the test unit and reliability and integrity of the complete

Table 2
Major elemental composition of seawater and reverse osmosis brine

Parameters/Unit	Seawater	SWRO brine
Total dissolved solids, mg/L	45,377	54,900
pH	7.3	7.13
Conductivity	58.3	69.4
Alkalinity as $CaCO_3$, mg/L	131.6	175
Boron, mg/L	3.7	9.8
Calcium, mg/L	730	1,090
Chloride, mg/L	24,876	35,212
Lithium, mg/L	–	1.7
Magnesium, mg/L	1,325	1,673
Potassium, mg/L	316.4	997
Sodium, mg/L	14,488.5	17,905
Strontium, mg/L	14.6	121
Sulfate, mg/L	3,430.5	4,159

Table 1
Commercially available aquaporin membrane and properties

Membrane type	Flat sheet	Flat sheet
Manufacturer	Aquaporin	Z-nano
Membrane thickness	110 μm (+/– 15 μm)	110 μm (+/– 15 μm)
Water channel	Aquaporin protein	Aquaporin protein
Test conditions	H_2O vs. 1 M NaCl; FO mode	H_2O vs. 1 M NaCl; FO mode
Water flux	>7 L/m^2·h	>7 L/m^2·h
NaCl reverse flux	<2.5 g/m^2·h	–
Operating conditions	Temp. range: 5°C–50°C Short-term exposure: 65°C pH range: 2–11 (Short-term exposure)	–

system. The schematic representation and actual image of the laboratory FO unit is shown in Fig. 1.

2.2. Characterization of aquaporin and Z-nano biomimetic membrane

Aquaporin and Z-nano membrane hydrophilicity was characterized by water contact angle (WCA) using Goniometer. EVO MA18 with Oxford EDS (X-act) field-emission scanning electron microscopy (FESEM) instrument was used to study the surface morphology of the membranes and the membrane surface topological features were analyzed using Nano-Observer atomic force microscopy (AFM) instrument by scanning the membrane 10 μm x 10 μm dimensions.

2.3. Experimental procedure for forward osmosis experiments

FO experiments were conducted using laboratory-scale cross flow filtration unit. The cross-flow permeation cell is a plate-and-frame design with a rectangular channel on each side of the membrane. The flow velocities of solutions during the FO testing were kept at constant values for both the FS and DS. The FS and DS were circulated in to membrane using concurrent flow technique. The constant temperatures of the FS and DS were maintained. NaCl solutions with different concentrations were prepared and used as the DS. Deionized (DI) water and aqueous NaCl solutions, seawater, and RO brine were used as the FS. During FO tests, the dilution of the DS is ignored, because the ratio of water permeation flux to the volume of the DS is less than 2%. In the FO test, the active layer of membrane was facing the FS. To record weight and conductivity changes, a digital mass balance and a conductivity meter was used. Each experiment was conducted for 120 min in triplicate, and mean values were reported. J_v and J_s values were calculate according to the following equation:

$$J_v = \frac{\Delta V}{A_m \cdot \Delta t} \tag{1}$$

where J_v is the water flux, ΔV is the volume change of FS, and A_m is the membrane effective area, Δt is time interval.

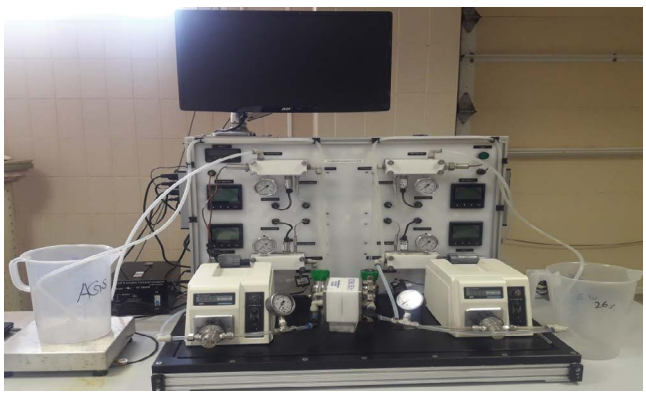

Fig. 1. Laboratory-scale forward osmosis instrument.

3. Results and discussion

3.1. Characterization

3.1.1. Water contact angle and water uptake studies of aquaporin and Z-nano membranes

The WCA of aquaporin and Z-nano membranes was measured using optical WCA and interface tension meter from USA KINO (model-SL200KB), in accordance with the sessile droplet method. The water uptake study of the membranes was measured by water uptake capacity using a standard protocol given in the literature [28].

It was observed that the WCA of aquaporin membrane was lower than the Z-nano membrane. But Z-nano membrane showed higher water uptake capacity than the aquaporin membrane as shown in Table 3. These variations in the WCA and water uptake capacity of membrane may be due to method of fabrication of biomimetic aquaporin protein and its chemical compositions.

3.1.2. Morphological and topological studies of aquaporin and Z-nano membranes

The water flux and antifouling character of membrane directly depend on the surface morphology and its topological features. The FESEM and AFM are considered the prominent technique to study the morphological and topological variation of membrane. FESEM image showed that the Z-nano membrane showed smaller and uniformly distributed pores compared with aquaporin membrane as shown in Fig. 2a. On the other hand, AFM image of Z-nano membrane showed lower roughness parameter compared with aquaporin membrane as shown in Fig. 2b. The surface roughness parameters are presented in Table 4, by means of the maximum mean roughness (R_a), root mean square roughness (R_q), and maximum feature height (R_{max}).

3.2. Desalination performance study of aquaporin and Z-nano membrane

The FO desalination experiments were conducted using flat sheet aquaporin and Z-nano membranes. The effect of osmotic pressure difference, flow rate and temperature on the water flux and water recovery was studied.

3.2.1. Effect of draw solution and feed solution concentration on water flux and water recovery for aquaporin and Z-nano membrane

The effect of DS and FS concentration on water flux was studied at constant flow rate of 500 mL/min and temperature 25°C for aquaporin and Z-nano membrane. The NaCl

Table 3
Water contact angle and water uptake capacity of aquaporin, and Z-nano membranes

Membrane code	WCA (°)	Water uptake capacity (%)
AqZ	24.83 ± 0.5	53.96 ± 0.4
Z-nano	59.33 ± 0.3	80.00 ± 0.5

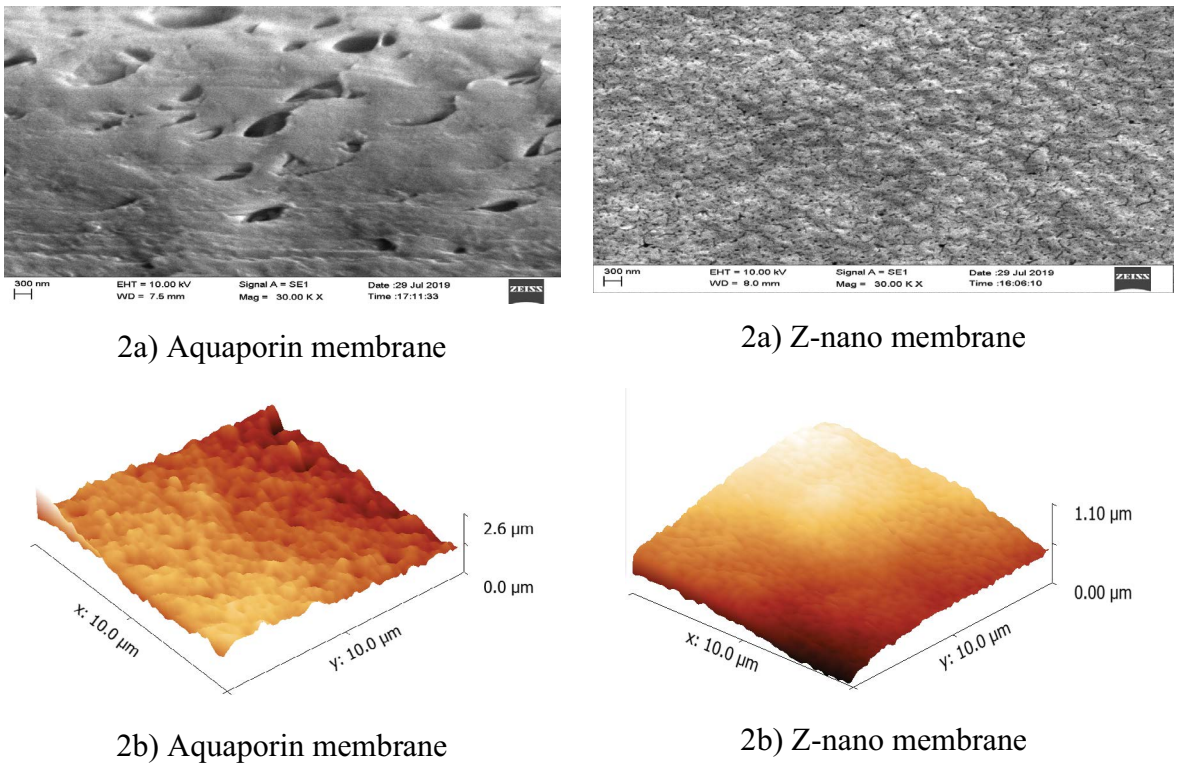

Fig. 2. (a) Magnified surface field-emission scanning electron microscopy image and (b) three-dimensional AFM images aquaporin and Z-nano membrane.

Table 4
Surface roughness parameters of aquaporin and Z-nano membrane

Membrane code	R_a (nm)	R_{ms} (nm)	R_{max} (nm)	Average (nm)
AqZ	60 ± 0.03	89 ± 0.05	2,601 ± 0.03	315 ± 0.03
Z-nano	186 ± 0.10	221 ± 0.20	1,103 ± 0.15	618 ± 0.15

Maximum mean roughness (R_a), root mean square roughness (R_q) and maximum feature heights (R_{max}).

DS concentrations were varied from 0.5, 3.5, 7.0, 15, and 26 wt.%, whereas FS concentration were varied from 0.5, 3.5, and 7.0 wt.% NaCl. The beach well (BW) seawater and RO brine were also used as feed. The result indicates that the water flux and water recovery was in proportion with FS concentration, as shown in Figs. 3 and 4, respectively. Maximum water flux was seen with 26 wt.% NaCl DS concentrations, which may be owing to its higher osmotic pressure compared to sodium chloride (NaCl) solutions with a lower concentration. The maximum water flux obtained for aquaporin membrane was 17.5 L/m²·h when DI water is used as FS and 26 wt.% NaCl is used as DS. The water flux of aquaporin membrane was 4.8 L/m²·h when 7 wt.% NaCl is used as FS and 26 wt.% NaCl is used as DS. The low water flux might be due to the reduced osmotic pressure differential between 7 wt.% NaCl FS and 26 wt.% NaCl DS.

The performance of Z-nano aquaporin membranes in desalination is superior to that of biomimetic aquaporin membranes. The trend is similar to aquaporin membrane performance, however, the higher water flux and water recovery was observed with Z-nano membrane. The maximum water flux measured for the Z-nano aquaporin membrane is approximately 78.6 L/m²·h for DI water FS and 26 wt.% NaCl DS concentration.

At 26 wt.% NaCl DS concentration, the Z-nano membrane demonstrated good water flux for seawater and RO brine FS also. The water flow for seawater FS was 57.9 and 23.7 L/m²·h for RO brine FS. The effect of FS and DS concentration on water flux and recovery for the aquaporin and Z-nano membranes are shown in Figs. 3 and 4.

3.2.2. Effect of flow rate on water flux and water recovery for aquaporin and Z-nano membrane

The effect of flow rate on water flux and water recovery for flat sheet aquaporin and Z-nano membranes were conducted using 26 wt.% NaCl DS and DI water, 0.5, 3.5, and 7.0 wt.% NaCl solutions, BW seawater and RO brine as feed. Experiments were conducted at 25°C and the flow rate of FS and DS were varied (500, 750, and 1,000 mL/min). The effect of flow rate on water flux and water recovery is shown in Figs. 5 and 6, respectively. The result shows that the water flux increased with increase of flow rate from 500 to 750 mL/min, but further increase of flow rate to 1,000 mL/min decreased the water flux for aquaporin membrane as shown in Fig. 5. It is clear from Fig. 5 that the water flux of aquaporin membrane was highest at 750 mL/min flow for all the FS. The highest water flux for aquaporin membrane

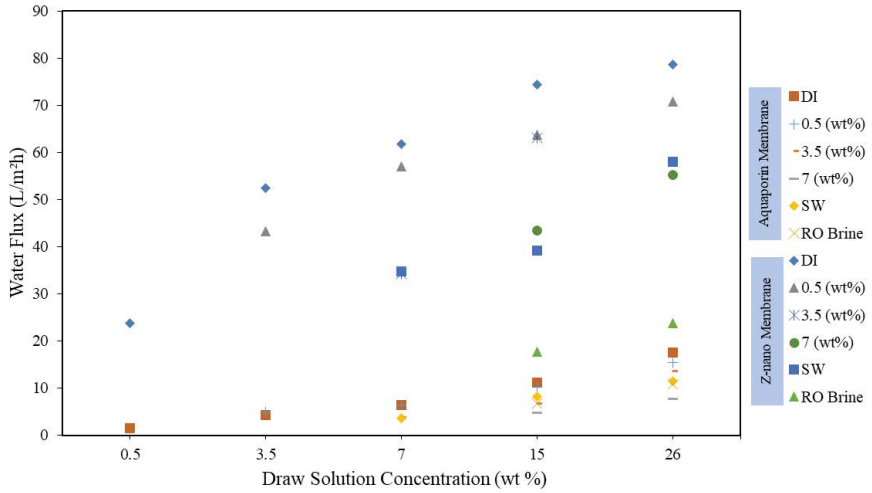

Fig. 3. Effect of FS and DS concentration on water flux for aquaporin and Z-nano membrane.

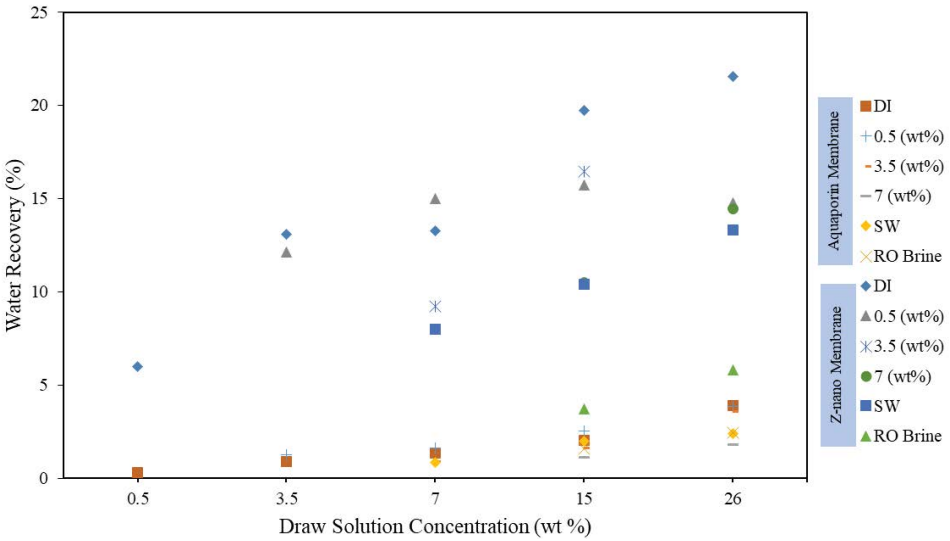

Fig. 4. Effect of FS and DS concentration on water recovery for aquaporin and Z-nano membrane.

observed was 24.4 L/m²·h for DI water feed and 18.8 L/m²·h for BW feed. The water recovery also showed the same trend observed with the water flux of aquaporin membrane; the maximum water recovery was 6.3% for DI water FS and 4.6% for BW FS at 750 mL/min flow rate.

The water flux and water recovery of Z-nano membrane increased with increase of flow rate from 500 to 1,000 mL/min for all the tested feed samples. On the other hand, water flux was decreased with increase of feed concentration. The higher water flux observed for Z-nano membrane is 71.84 L/m²·h and corresponding water recovery is 15.6%. Actual desalination performance using seawater and RO brine as a feed also showed excellent results. The water flux was 58.1 L/m²·h for seawater feed and 34.5 L/m²·h for RO brine feed at 1,000 mL/min flow rate. In comparison, Z-nano membrane showed 2–6 times higher water flux and recovery than aquaporin membrane with BW seawater and DI water feed, respectively.

3.2.3. Effect of temperature on water flux and water recovery for aquaporin and Z-nano membrane

The effect of temperature on water flux and water recovery for flat sheet aquaporin and Z-nano membranes were conducted using 26 wt.% NaCl DS and DI water, 0.5, 3.5, and 7.0 wt.% NaCl solution, BW and RO brine as feed. Experiments were conducted at flow rate of 500 mL/min and the temperature was varied (15°C, 25°C, and 40°C). As shown in Figs. 7 and 8, the water flux and water recovery increased with increase in temperature from 15°C to 40°C for all the tested feed samples and membranes. The maximum water recovery for aquaporin membrane was 5.4% for DI water FS at 40°C; the corresponding water flux was 22.0 L/m²·h. The increase of water flux with increase of temperature is due to increased osmotic pressure and diffusion co-efficient and decrease of viscosity at higher temperature. The maximum water flux of 17.5 and 15.4 L/m²·h

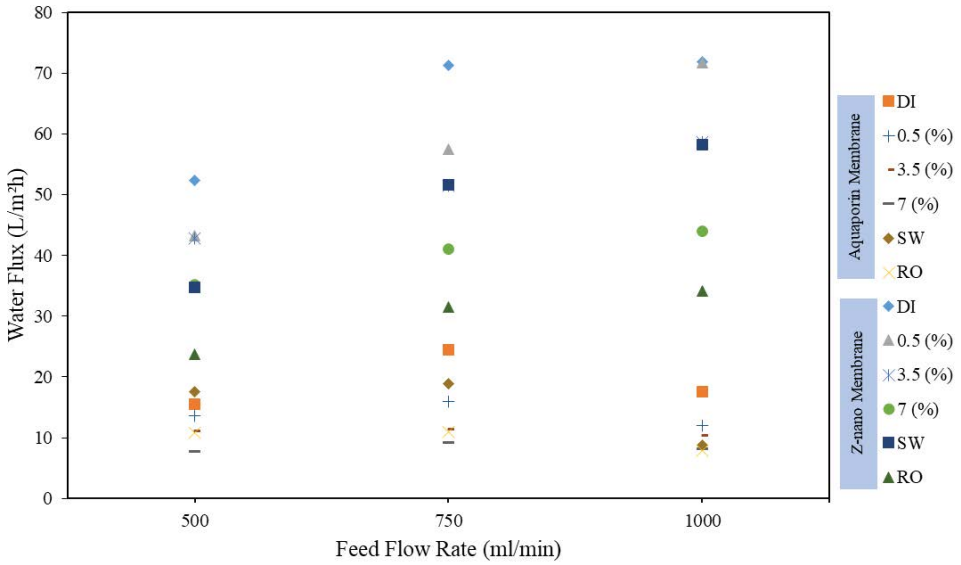

Fig. 5. Effect of flow rate on water flux for aquaporin and Z-nano membrane.

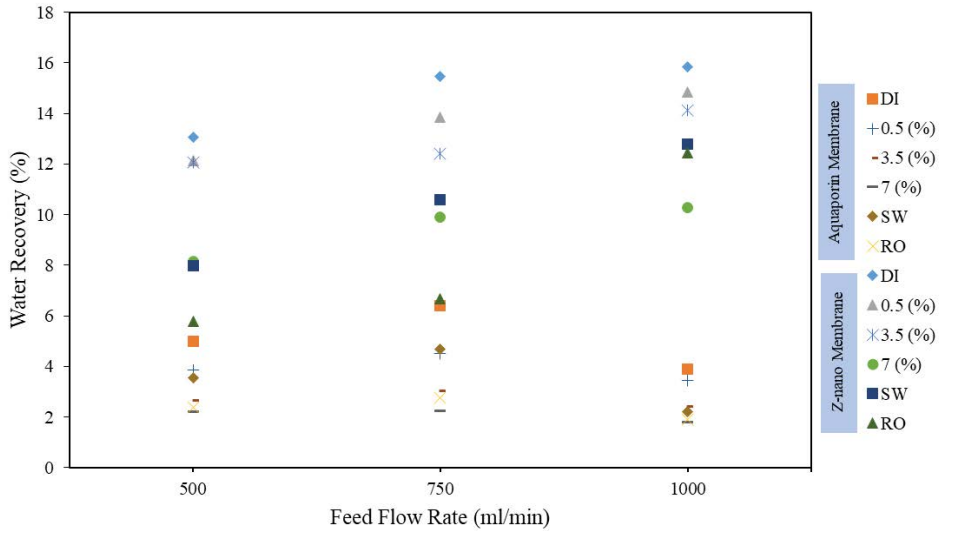

Fig. 6. Effect of flow rate on water recovery for aquaporin and Z-nano membrane.

was observed for BW and RO brine as FS using 26 wt.% DS for aquaporin membrane. For all the FS, 40°C temperature showed very promising and excellent results in terms of water flux and water recovery. The maximum water flux observed for Z-nano membrane was 54.4 L/m²·h, and corresponding water recovery is 13.0%. The maximum water flux observed for seawater and RO brine FS are 34.7 and 23.7 L/m²·h respectively as shown in Figs. 7 and 8.

While comparing the desalination performance of aquaporin and Z-nano membranes, the Z-nano membranes performed significantly better than the aquaporin membranes. For all the membranes, increasing the DS concentration led to an increase in the water flux and water recovery percentage, while increasing the FS concentration led to a decrease in both these values. The highest water flux that was measured was around 78.6 L/m²·h for DI water FS when the DS concentration was 26 wt.% for the Z-nano membrane. Additionally, the Z-nano membrane demonstrated an outstanding water flux for seawater and RO brine FS using 26 wt.% NaCl DS. When compared to the aquaporin membrane, the water flux that was observed for Z-nano membranes was significantly higher throughout this study. This enhanced water permeability is may be due to better water uptake capacity, morphological and topological features of the Z-nano membrane.

3.3. Desalination performance comparison of biomimetic and non-biomimetic membranes

Using seawater and RO brine as FS, the desalination performance of commercially available cellulose triacetate (CTA) and thin-film composition (TFC) membranes

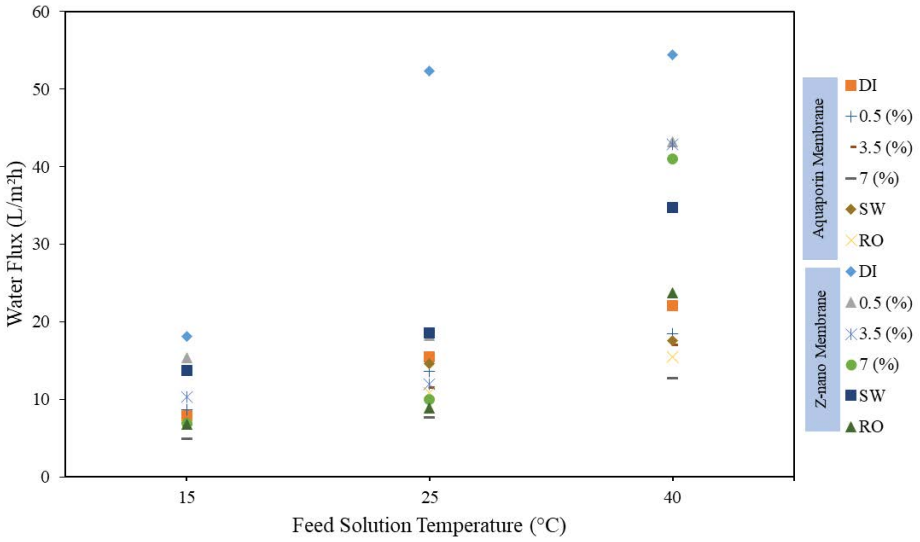

Fig. 7. Effect of temperature on water flux for aquaporin and Z-nano membrane.

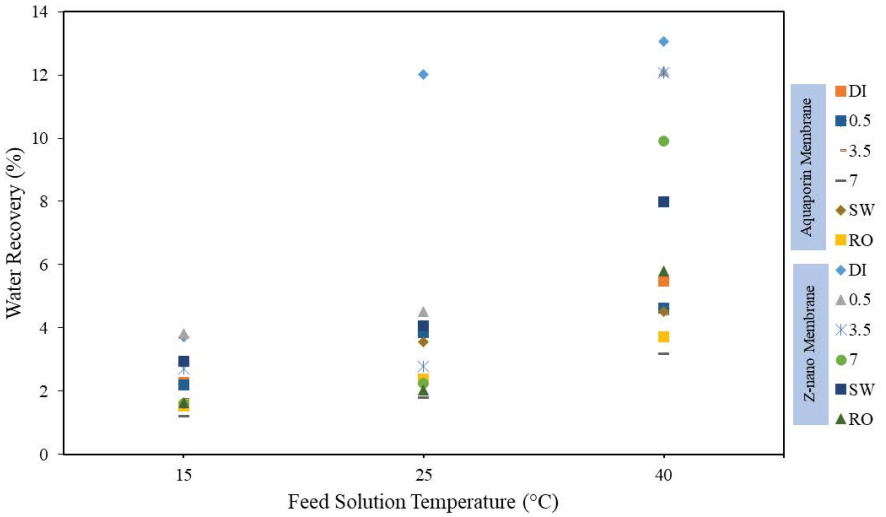

Fig. 8. Effect of temperature on water recovery for aquaporin and Z-nano membrane.

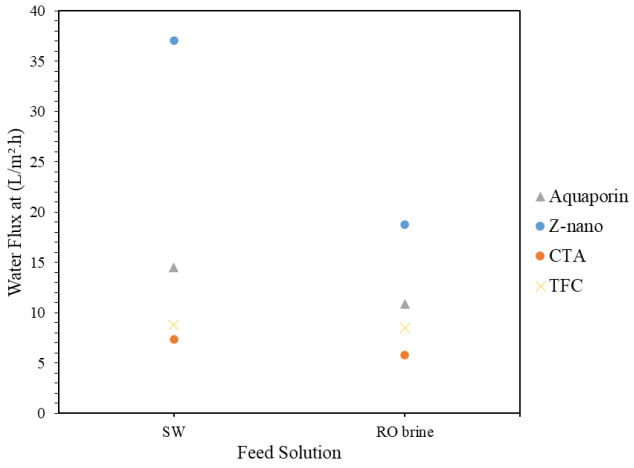

Fig. 9. Water flux of aquaporin, Z-nano, CTA and TFC membrane.

was investigated. Flow rate, temperature, and DS concentrations were kept constant at 500 mL/min, 25°C, and 26 wt.%, respectively. Fig. 9 compares water flux between biomimetic (aquaporin and Z-nano) and non-biomimetic (CTA and TFC) membranes. When compared to the other studied membranes, the Z-nano membrane had the highest water flux. The water flux order for the tested membranes is Z-nano > aquaporin > TFC > CTA. Fig. 8 shows that biomimetic membranes are more effective than non-biomimetic membranes for desalinating seawater and RO brine. This improved performance could be attributed to the presence of aquaporin water channels in biomimetic membranes.

4. Conclusion

Research on the efficiency of biomimetic FO membrane was carried out by varying the concentrations of FS and DS, as well as the flow rate and temperature. The findings of

the experiments showed that an increase in the flow rate, temperature, and concentration of the DS led to an increase in the water flux as well as an increase in the water recovery. On the other hand, water flux and water recovery both reduced as FS concentration increased. The results from the experiments that were conducted on the Z-nano membrane using 26 wt.% sodium chloride DS showed a maximum water flux of 58.1 L/m^2·h for seawater and 34.2 L/m^2·h for RO brine FS, respectively at a flow rate of 1,000 mL/min and at 25°C. When compared with Z-nano membrane, biomimetic aquaporin membrane consistently exhibited lower water flux and water recovery ratio for all of the conditions that were examined. While comparing biomimetic and non-biomimetic membranes, water flux obtained was in the order Z-nano (biomimetic) > aquaporin (biomimetic) > TFC (non-biomimetic) > CTA (non-biomimetic). Aquaporin biomimetic membranes exhibited water flux almost 2 times higher than CTA and TFC membranes. In comparison, Z-nano biomimetic membrane demonstrated 2–5-fold higher water flux than CTA and TFC membrane. This improved performance could be explained by the presence of aquaporin water channels in biomimetic membranes. The findings of the laboratory-scale FO tests indicate that the Z-nano membrane is better suited to achieve a higher water flux and water recovery ratio while using RO brine and seawater as the FS. As a result, biomimetic membranes are more suitable for seawater desalination, desalination brine concentration, and industrial waste water treatment. The study suggests testing biomimetic membranes on a pilot scale to assess energy usage and fouling behavior.

Acknowledgements

Authors are thankful to the Kuwait Institute for Scientific Research (KISR) for funding and supporting the implementation of this research work.

References

[1] M.F. Al-Rashed, M.M. Sherif, Water resources in the GCC countries: an overview, Water Resour. Manage., 14 (2000) 59–75.
[2] G.O. Odhiambo, Water scarcity in the Arabian Peninsula and socio-economic implications, Appl. Water Sci., 7 (2017) 2479–2492.
[3] H.E.S. Fath, A.S. Hassan, T. Mezher, Present and future trend in the production and energy consumption of desalinated water in GCC countries, Int. J. Therm. Environ. Eng., 5 (2013) 155–165.
[4] A. Panagopoulos, Water-energy nexus: desalination technologies and renewable energy sources, Environ. Sci. Pollut. Res., 28 (2021) 21009–21022.
[5] A. Panagopoulos, V. Giannika, Comparative techno-economic and environmental analysis of minimal liquid discharge (MLD) and zero liquid discharge (ZLD) desalination systems for seawater brine treatment and valorization, Sustainable Energy Technol. Assess., 53 (2022) 102477, doi: 10.1016/j.seta.2022.102477.
[6] A. Panagopoulos, Brine management (saline water & wastewater effluents): sustainable utilization and resource recovery strategy through minimal and zero liquid discharge (MLD & ZLD) desalination systems, Chem. Eng. Process. Process Intensif., 176 (2022) 108944, doi: 10.1016/j.cep.2022.108944.
[7] A. Panagopoulos, Techno-economic assessment and feasibility study of a zero liquid discharge (ZLD) desalination hybrid system in the Eastern Mediterranean, Chem. Eng. Process. Process Intensif., 178 (2022) 109029, doi: 10.1016/j.cep.2022.109029.
[8] P.G. Nicoll, Forward Osmosis – A Brief Introduction, The International Desalination Association World Congress on Desalination and Water Reuse, Tianjin, China, 2013.
[9] H. Wang, T.-S. Chung, Y.W. Tong, K. Jeyaseelan, A. Armugam, Z. Chen, M. Hong, W. Meier, Highly permeable and selective pore-spanning biomimetic membrane embedded with aquaporin Z, Small, 8 (2012) 1185–1190.
[10] P. Gena, M. Pellegrini-Calace, A. Biasco, M. Svelto, G. Calamita, Aquaporin membrane channels: biophysics, classification, functions, and possible biotechnological applications, Food Biophys., 6 (2011) 241–249.
[11] A. Taubert, Controlling water transport through artificial polymer/protein hybrid membranes, Proc. Natl. Acad. Sci. U.S.A., 104 (2007) 20643–20644.
[12] A. Engel, Y. Fujiyoshi, T. Gonen, T. Walz, Junction-forming aquaporins, Curr. Opin. Struct. Biol., 18 (2008) 229–235.
[13] J. Heo, F. Meng, S.Z. Hua, Contribution of aquaporins to cellular water transport observed by a microfluidic cell volume sensor, Anal. Chem., 80 (2008) 6974–6980.
[14] J.S. Hub, B.L. de Groot, Mechanism of selectivity in aquaporins and aquaglyceroporins, Proc. Natl. Acad. Sci. U.S.A., 105 (2008) 1198–1203.
[15] C.-X. Zhao, H.-B. Shao, L.-Y. Chu, Aquaporin structure-function relationships: water flow through plant living cells, Colloids Surf., B, 62 (2008) 163–172.
[16] M. Kumar, M. Grzelakowski, J. Zilles, M. Clark, W. Meier, Highly permeable polymeric membranes based on the incorporation of the functional water channel protein aquaporin Z, Proc. Natl. Acad. Sci. U.S.A., 104 (2007) 20719–20724.
[17] P. Agre, The aquaporin water channels, Proc. Am. Thorac. Soc., 3 (2006) 5–13.
[18] J.R. Werber, C.O. Osuji, M. Elimelech, Materials for next-generation desalination and water purification membranes, Nat. Rev. Mater., 1 (2016) 16018, doi: 10.1038/natrevmats.2016.18.
[19] C.Y. Tang, Y. Zhao, R. Wang, C. Hélix-Nielsen, A.G. Fane, Desalination by biomimetic aquaporin membranes: review of status and prospects, Desalination, 308 (2013) 34–40.
[20] Y. Li, Q. Saren, T. Miao, W. Wentalia, W. Rong, Fabrication of aquaporin-based biomimetic membrane for seawater desalination, Desalination, 467 (2019) 103–112.
[21] H.T. Madsen, N. Bajraktari, C. Hélix-Nielsen, B. Van der Bruggen, E.G. Søgaard, Use of biomimetic forward osmosis membrane for trace organics removal, J. Membr. Sci., 476 (2015) 469–474.
[22] A. Beratto-Ramos, J. Dagnino-Leone, J. Martínez-Oyanedel, M. Aranda, R. Bórquez, Fabrication and filtration performance of aquaporin biomimetic membranes for water treatment, Sep. Purif. Rev., 51 (2022) 340–357.
[23] M. Ahmed, R. Kumar, Y. Al-Wazzan, B. Garudachari, J.P. Thomas, Assessment of performance of inorganic draw solutions tested in forward osmosis process for desalinating Arabian gulf seawater, Arabian J. Sci. Eng., 43 (2018) 6171–6180.
[24] M. Ahmed, R. Kumar, B. Garudachari, J.P. Thomas, Assessment of pilot scale forward osmosis system for Arabian Gulf seawater desalination using polyelectrolyte draw solution, Desal. Water Treat., 157 (2019) 342–348.
[25] R. Kumar, M. Ahmed, B. Garudachari, J.P. Thomas, Evaluation of the forward osmosis performance of cellulose acetate nanocomposite membranes, Arabian J. Sci. Eng., 43 (2018) 5871–5879.
[26] R. Kumar, M.M. Ahmed, B. Garudachari, J.P. Thomas, Synthesis and evaluation of nanocomposite forward osmosis membranes for Kuwait seawater desalination, Desal. Water Treat., 176 (2020) 273–279.
[27] M. Ahmed, Y. Al-Wazzan, R. Kumar, B. Garudachari, J.P. Thomas, A comparative study of two different forward osmosis membranes tested using pilot-plant system for Arabian gulf seawater desalination, Desal. Water Treat., 176 (2019) 252–259.
[28] R.S. Hebbar, A.M. Isloor, A. Ismail, S.J. Shilton, A. Obaid, H.-K. Fun, Probing the morphology and anti-organic fouling behaviour of a polyetherimide membrane modified with hydrophilic organic acids as additives, New J. Chem., 39 (2015) 6141–6150.